02,11

Phase transformations in barium-strontium niobate SBN-50 in the temperature range from 80 K to 700 K according to Raman spectroscopy data

© YaYu. Matyash, A. S. Anokhin, A.V. Pavlenko

Southern Scientific Center, Russian Academy of Sciences, Rostov-on-Don, Russia

E-mail: matyash.ya.yu@gmail.com

Received June 8, 2022
Revised June 8, 2022
Accepted June 12, 2022

The lattice dynamics of the $Sr_{0.5}Ba_{0.5}Nb_2O_6$ (SBN-50) ceramic was studied using Raman spectroscopy in the temperature range of 80−700 K with a step of 10 K. The analysis of the Raman spectra in the range $\nu = 50-1000\,cm^{-1}$ revealed features in the temperature dependence behavior of the optical modes frequencies associated with the displacement of Ba, Sr and Nb atoms from their average positions in the crystal lattice, which is associated with a macroscopic phase transition from the paraelectric to the ferroelectric phase in the vicinity of 390 K. It is shown that anomalies at $T \sim 565$ K on the temperature dependences of the frequency and line half-width corresponding to the oscillations of the NbO_6 octahedron can be caused by the presence of polar nanoregions in the paraelectric phase in SBN-50. When the sample was cooled to a temperature of 80 K, the behavior was recorded in the Raman spectra, indicating the occurrence of a structural phase transition in the ferroelectric phase in the vicinity of 190 K. The reasons for the revealed patterns are discussed.

Keywords: ferroelectric, Raman scattering, SBN, tetragonal tungsten bronze.

DOI: 10.21883/PSS.2022.11.54181.402

1. Introduction

Solid solutions (SS) of barium strontium niobate, $Sr_xBa_{1-x}Nb_2O_6$ (SBN), belong to the group of ferroelectric (FE)-relaxors with a structure of unfilled tetragonal tungsten bronze (TTB) [1] in a concentration interval of $x = 0.25-0.75$. General structural formula is $(A1, A2)_6C_4(B1_2B2_8)O_{30}$. TTB structure consists of a framework of bound octahedra of NbO_6, that form three types channels with different symmetry along the c axis: section A1 (inside square channels) is occupied by Sr atoms, section A2 (inside pentagonal channels) is occupied by Sr and Ba, and section C (inside triangle channels) is empty. The partial filling of channels in a real SBN structure results in disordering, which is a source of many unusual properties [2]. Some SS of SBN have high electrooptic coefficients, photorefractive effect [3], as well as significant pyroelectric and piezoelectric properties [4–6] that make them promising materials for application in modern functional microelectronics and optoelectronic devices [7]. Despite the extensive studying of barium strontium niobates for more than 50 years, currently the issues related to understanding the nature of relaxor properties manifestation, mechanisms of spontaneous polarization emergence and phase transformations in them remain pending.

The lattice dynamics at FE phase transition (PT) in SBN is affected by many factors, one of which, according to the Raman spectroscopy data [8], is the ratio of Ba/Sr. The analysis of temperature behavior of individual lines (near $630\,cm^{-1}$) in the Raman spectra reported in [9] has shown an almost linear decrease in the Curie temperature (Tc) with an increase in Sr content, that was correlated with the dielectric spectroscopy data [10]. In SBN-50 and SBN-75 crystals at room temperature A_1(TO), E(TO), E(LO), B_1, B_2 modes were identified, as well as longitudinal (QL) and transverse (QT) modes [11]. Monotonous changes of mode frequencies depending on temperature were found in the SBN-50 crystal [12], a similar behavior of low-frequency modes near FE PT was observed in SBN-61 [13]. PT in SBN-61 and SBN-75 single crystals, as well as possible causes of the difference in the quantity of theoretically predicted and experimentally obtained modes were described in [14]. By the present, many research teams have performed a number of papers devoted to the studying of the structure, lattice dynamics of SBN-x in various executions, determining the mechanism(s) of PT in these materials. However, most often these studies are segmental and carried out in a limited temperature range, that makes impossible to get a holistic view of the barium strontium niobate lattice dynamics evolution and to find out experimentally the sequence of phase transformations in them, which is the goal of this study.

2. Samples. Methods of obtaining and research

The SBN-50 ceramics was made from $SrCO_3$, $BaCO_3$ carbonates and Nb_2O_5 oxide by solid-phase reactions followed

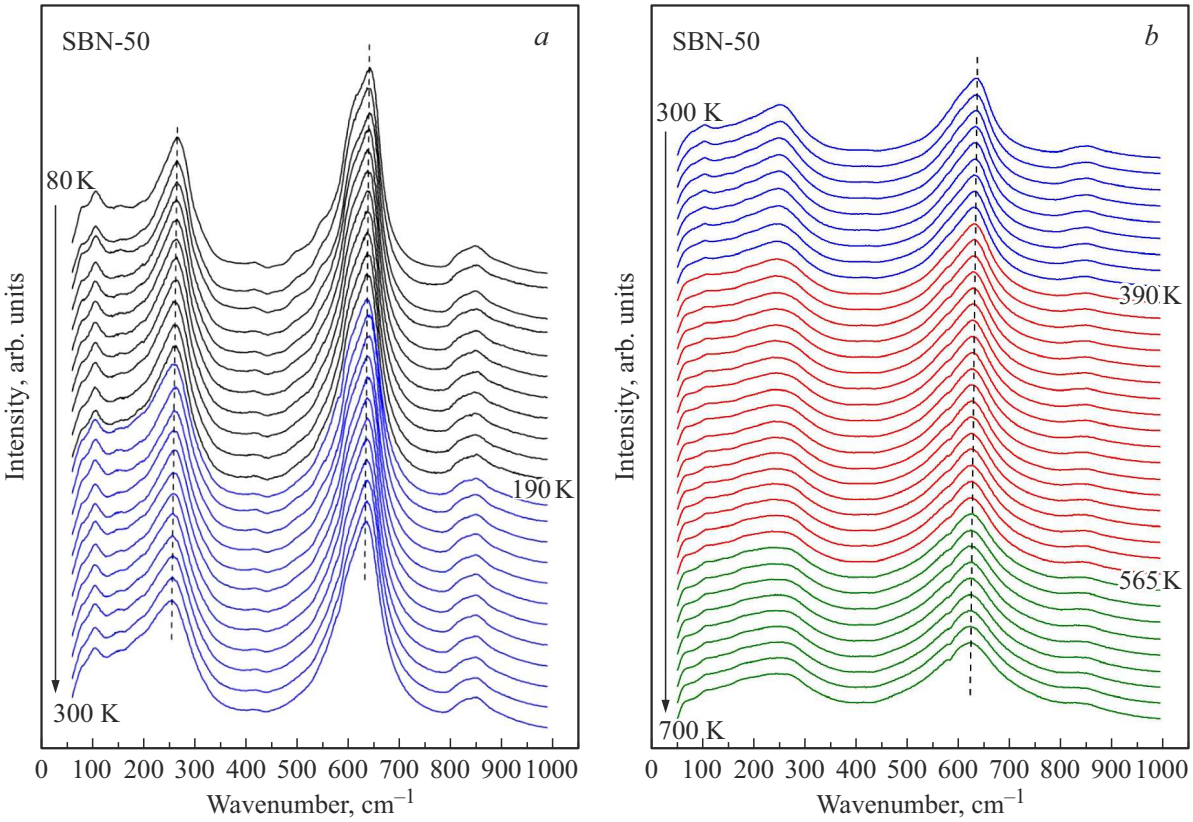

Figure 1. Temperature dependences of the Raman spectra of SBN-50 ceramics obtained by cooling (a) and heating (b).

by sintering using conventional ceramic technology in the Department of Intelligent Materials and Nanotechnologies of the Research Institute of Physics of the Southern Federal University (Rostov-on-Don). The ceramics was characterized by tetragonal symmetry with the lattice cell parameters: $a = 1.2355$ nm and $c = 0.3896$ nm [6].

To obtain Raman spectra, we used polarized radiation of an argon laser ($\lambda = 514.5$ nm) and a Renishaw in Via Reflex micro-Raman spectrometer with an edge filter that allows recording spectra starting from 50 cm^{-1} The spectra were recorded according to the backscattering scheme using a Leica optical microscope, the diameter of the laser beam on the sample was $1-2\,\mu$m. Temperature measurements were performed using a Linkam THMS600 cryostat/furnace (with a thermal stability of $\sim 0.01°$K). The spectra were obtained in the cooling mode from 300 to 80 K and in the heating mode from 300 to 700 K. The temperature step was 10 degrees, exposition at each temperature was 5 minutes.

3. Experimental results and discussion

Macroscopic PT from FE-state to PE-state is accompanied by a structural transition from the tetragonal phase with space group $P4bm$ to group $P4b2$. There are 138 possible vibration modes for space group $P4bm$, that can be represented in accordance with the following irreducible representations: $\Gamma_{vib} = 19A_1(R, IR) + 15A_2 + 14B_1(R) + 18B_2(R) + 36E(R, IR)$, where R and IR represent Raman and infrared active optical phonon modes, respectively. Three of these modes are acoustic modes, and all A_2 modes are inactive neither in Raman, nor in IR spectra. Thus, there are 120 active Raman modes, however, the number of experimentally observed lines is considerably less as compared with the theoretical forecasts [14], that, according to the majority of authors [2], is due to the cation disordering in the TTB structure. This, in turn, results in disturbances of the selection rules by a wave vector in the center of the Brillouin zone [13]. Also, a degeneration of some optical phonon modes into one band is possible, that promotes additional broadening of lines in the Raman spectra.

Fig. 1 shows the temperature Raman spectra recorded in a range of 80–700 K.

Parameters of individual phonons (peak position, half-width, area) were determined by the approximation of experimental spectrum by a set of additive non-interacting harmonic oscillators. Intensities of all obtained spectra were corrected for the Bose–Einstein temperature factor $n(\nu, T) = (\exp(h\nu/kT) - 1)^{-1}$. The approximated Raman spectrum of the SBN-50 ceramics at 300 K is shown in Fig. 2.

An attention should be paid to the lines that give the largest contribution to the intensity of the ceramics

spectrum (101, 256, 600, 636 and 856 cm^{-1}). The line at 101 cm^{-1} corresponds to vibrations of Ba and Sr cations in pentagonal and tetragonal channels, the mode at 256 and 856 cm^{-1} corresponds to deformation oscillations of O–Nb–O. The band of $\sim$ 630 cm^{-1} is a combination of two optical phonons (600 and 636 cm^{-1}) and corresponds to valence oscillations of the NbO_6 octahedron. However, it is difficult to identify oscillations in more details, because all internal modes of NbO_6 octahedra are located too close to see them in the Raman spectra even at low temperatures. As it was mentioned before, the strong disordering in the structure of SBN-50 ceramics results in broadening of lines, which, in turn, limits the number of observed features in the Raman spectra as well. The temperature dependence of optical mode frequencies (Fig. 3) demonstrates several obvious features. Firstly, for the intense line near 636 cm^{-1}, the shape of the temperature dependence of frequency changes in Raman spectra when the temperature of $\sim$ 565 K is achieved. Secondly, frequencies of lines in a range of 70–300 cm^{-1} decrease sharply when the sample is heated over 380 K. Another feature can be seen at a temperature of $\sim$ 190 K: the band at 505 cm^{-1} is split into two lines (507 and 545 cm^{-1}) while further cooling the SBN-50; frequency of the line at 563 cm^{-1} increases, while the line at 702 cm^{-1} demonstrates an inverse dependence, i.e,. decrease in frequency. The following is the detailed consideration of each feature. In the SBN structure crystallographic sites B1 and B2, occupied by atoms of Nb, denote different symmetry. Accordingly, the contribution to the macroscopic polarization from Nb(1) and Nb(2) atoms will be different. Displacements of Me (Ba, Sr and Nb) atoms from middle oxygen layers in the direction normal to the tetragonal axis z result in ferroelectric polarization [2,8]. Of interest in the Raman spectra is the line at 636 cm^{-1}, the phonons of this line are polarized along the z axis, in the direction of which, according to [14], atoms in SBN (the NbO_6 octahedron) are displaced during the FE PT.

However, in our case broadening of the line at 636 cm^{-1} and the change in the slope of the temperature dependence of the frequency and half-width for the line at 636 cm^{-1} changes in the PE phase near 565 K. Also, similar anomalies above the PT temperature were observed in the dependences of deformations [15], elastic modulus and the signal of second harmonics generation (SHG) [16] for SBN-x crystals ($x = 0.33$, 0.5, 0.61, and 0.75). The features detected by different methods may be associated with the formation of local polar regions in the SBN-50 ceramics at temperatures above the PT.

It should be noted, that currently there is no definite opinion in literature regarding the type of PT in SBN. Studies by dielectric, Raman and IR spectroscopies show that there are features in the SBN structures, which are typical for both the PT displacement type and the order-disorder type [8]. A feature of behavior of 7 lines in a range of 70–300 cm^{-1} is shown on the temperature dependence of optical mode frequencies. Some of the lines under consideration correspond to oscillations of Sr and Ba

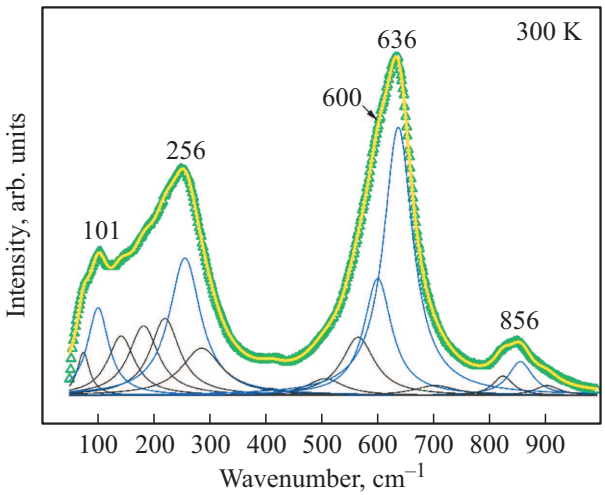

Figure 2. Decomposition of the SBN-50 ceramics Raman spectrum at 300 K.

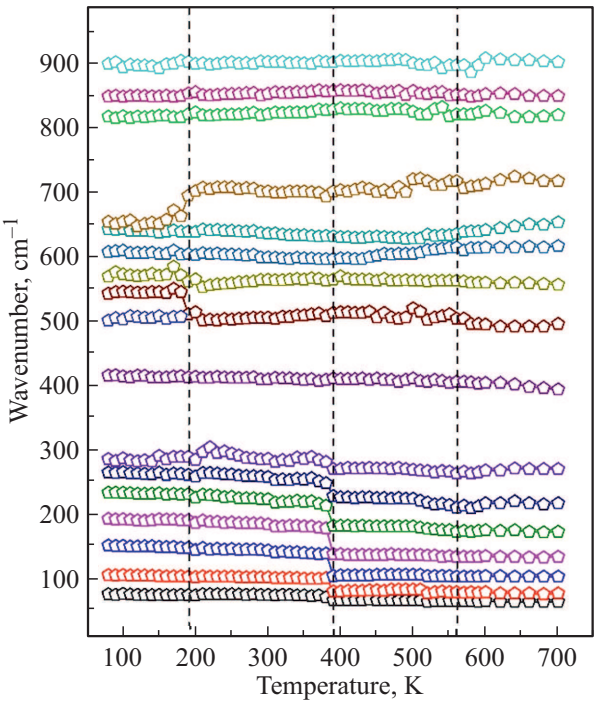

Figure 3. Temperature dependences of optical mode frequencies for SBN-50 ceramics.

cations in channels [17], other correspond to deformation oscillations of O–Nb–O (the mode at 256 cm^{-1}). With the temperature increase over 380 K a broadening of lines is observed in Raman spectra, as well as a sudden jump of all these lines to the low-frequency region, which is indicative of PT from the tetragonal phase $P4bm$ to $P4b2$ at $\sim$ 390 K.

The PT temperature found in this study is confirmed by the data of other methods, in particular, in [15,16,18] devoted to crystals and ceramics of SBN-50. When the ceramics is cooled below 200 K, also some anomalies are

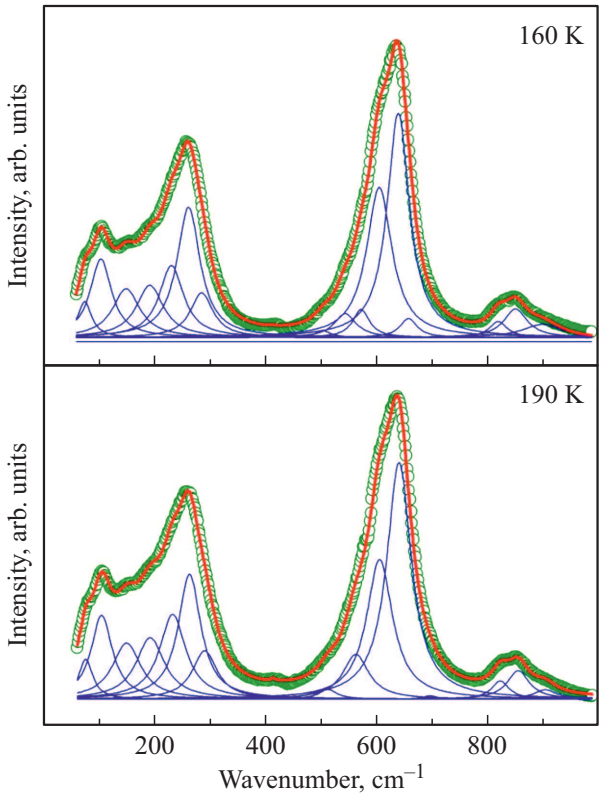

Figure 4. Approximated Raman spectra of SBN-50 ceramics near the temperatures of the third anomaly.

observed in Raman spectra (Fig. 4) and on the temperature dependence of optical mode frequencies.

When the sample is cooled to a temperature of 190 K, in the Raman spectra the 505 cm^{-1} mode split into two: 507 and 545 cm^{-1}, lines at 563 and 702 cm^{-1} shift towards higher and lower frequencies, respectively. All these features are indicative of a structural PT in the ferroelectric phase at this temperature. Unfortunately, our data is not enough to make an assumption on what phase is implemented in the process of this phase transformation. The performed study of temperature-frequency dependencies of relative permittivity and dielectric loss tangent in a frequency range of $0.1 - 1$ MHz confirmed the abnormal behavior at these temperatures as well. A similar PT was found in [19] at 198 K, where authors connected it with the emergence of an incommensurate structure in the crystal of $Sr_{0.5}Ba_{0.5}NbO_6$, that most likely takes place in our case as well.

4. Conclusion

Thus, in the SBN-50 ceramics in a range of 300–700 K a PT occurs at 390 K associated with the displacement of Ba, Sr, and Nb atoms from their mean sites. Temperature dependencies of frequencies and half-widths of lines show two clearly distinguished anomalies at $\sim$ 565 and $\sim$ 190 K. In the first, high-temperature case it can be assumed that features in Raman spectra are connected to the presence of polar nanoregions in the PE-phase. The second anomaly is the most likely indicative of the existence of low-temperature structural transition. It is reasonable to use the obtained results on phase transformations in the SBN-50 ceramics for the development of materials based on barium strontium niobates in the form of both ceramics and single crystals and thin films.

Funding

The work has been performed under the state assignment of the Southern Scientific Center of RAS, project No. 122020100294-9.

Conflict of interest

The authors declare that they have no conflict of interest.

References

[1] Yu.S. Kuz'minov. Ferroelectric crystals to control laser radiation. Nauka, M. (1982). 400 p. (in Russian).
[2] P.B. Jamieson, S.C. Abrahams, J.L. Bernstein. J. Chem. Phys. **48**, 5048 (1968).
[3] M.D. Ewbank, R.R. Neurgaonkar, W.K. Cory, J. Feinberg. J. Appl. Phys. **62**, *2*, 374 (1987).
[4] A.M. Glass. J. Appl. Phys. **40**, 4699 (1969).
[5] J. Dec, W. Kleemann, T. Woike, R. Pankrath. Eur. Phys. J. B **14**, *4*, 627 (2000).
[6] A.V. Pavlenko, A.G. Abubakarov, L.A. Reznichenko, I.M. Aliev, L.A. Shilkina, A.V. Nazarenko, I.A. Verbenko, G.M. Konstantinov. Technical Physics **85**, *8*, 80 (2015) (in Russian).
[7] M.C. Gupta. The Handbook of Photonics. CRC Press, Boca Raton. (1997). 768 p.
[8] E. Buixaderas, M. Pasciak. IEEE Trans. Ultrason. Ferroelectr. Freq. Control **68**, *2*, 314 (2021).
[9] A. Speghini, M. Bettinelli, U. Caldino, M.O. Ramirez, D. Jaque, L.E. Bausa, J. Garcia Sole. J. Phys. D **39**, *23*, 4930 (2006).
[10] J. Zhang, G. Wang, F. Gao, Ch. Mao, F. Cao, X. Dong. Ceram. Int. **39**, *2*, 1971 (2013).
[11] E. Amzallag, T.S. Chang, R.H. Pantell, R.S. Feigelson. J. Appl. Phys. **42**, *8*, 3254 (1971).
[12] K.G. Barlett, L.S. Wall. J. Appl. Phys. **44**, *11*, 5192 (1973).
[13] R.E. Wilde. J. Raman Spectrosc. **22**, *6*, 321 (1991).
[14] K. Samanta, A.K. Arora, T.R. Ravindran, S. Ganesamoorthy, K. Kitamura, S. Takekawa. Vib. Spectrosc. **62**, 273 (2012).
[15] A.S. Bhalla, R. Guo, L.E. Cross, G. Burns, F.H. Dacol, R.R. Neurgaonkar. Phys. Rev. B **36**, *4*, 2030 (1987).
[16] A.M. Pugachev, I.V. Zaytseva, V.K. Malinovsky, N.V. Surovtsev, M.V. Gorev, L.I. Ivleva, P.A. Lykov. Ferroelectrics **560**, *1*, 54 (2020).
[17] E. Buixaderas, I. Gregora, J. Hlinka, J. Dec, T. Lukasiewicz. J. Phase Transit. **86**, *2–3*, 217 (2013).
[18] L. Peng, K. Jiang, J. Zhang, Z. Hu, G. Wang, X. Dong, J. Chu. J. Phys. D **49**, *3*, 035307 (2016).
[19] L.A. Bursill, J.L. Peng. Acta Cryst. B **43**, 49 (1987).